PM$_{2.5}$-bound unresolved complex mixtures (UCM) in the Pearl River Delta region: Abundance, atmospheric processes and sources

Hua Fang [a,c], Scott D. Lowther [d], Ming Zhu [a,c], Chenglei Pei [e], Sheng Li [a,c], Zheng Fang [a,c], Xu Yu [a,c], Qingqing Yu [a,c], Yujun Wang [e], Yanli Zhang [a,b], Kevin C. Jones [d], Xinming Wang [a,b,c,*]

[a] State Key Laboratory of Organic Geochemistry and Guangdong Key Laboratory of Environmental Protection and Resources Utilization, Guangzhou Institute of Geochemistry, Chinese Academy of Sciences, Guangzhou, 510640, China
[b] Center for Excellence in Urban Atmospheric Environment, Institute of Urban Environment, Chinese Academy of Sciences, Xiamen, 361021, China
[c] University of Chinese Academy of Sciences, Beijing, 100049, China
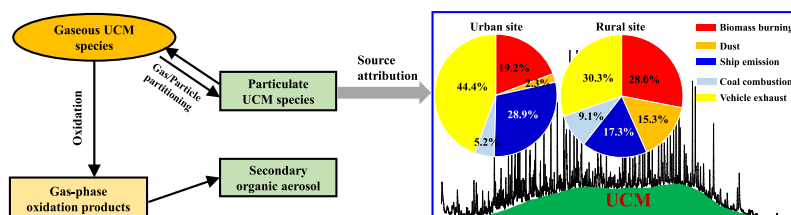[d] Lancaster Environment Centre, Lancaster University, Lancaster LA1 4YQ, United Kingdom
[e] Guangzhou Environmental Monitoring Center, Guangzhou, 510060, China

HIGHLIGHTS

- PM$_{2.5}$-bound unresolved complex mixtures (UCM) was characterized in the PRD region.
- Missing UCM in hot months for enhanced partition into gas phase, photo-oxidation and lower organic matter.
- UCM in cool months accounted for ~9% of PM$_{2.5}$ with over 30% UCM from vehicles exhaust.
- Biomass burning contributed up to 28% of UCM at the rural site.
- Ship emission contributed 29% UCM at the urban site and 17% UCM at the rural site.

GRAPHICAL ABSTRACT

ARTICLE INFO

ABSTRACT

Unresolved complex mixture (UCM) accounts for a substantial fraction of particulate organic matters and plays an important role in forming secondary organic aerosol (SOA), yet their abundance, sources and atmospheric processes are not well understood. In this study, filter-based ambient PM$_{2.5}$ samples were collected concurrently at an urban site and a rural site in the Pearl River Delta (PRD) region, south China, to characterize semi-volatile UCM. Dust, urban tunnel exhaust, ship exhaust and biomass burning samples were also collected to characterize UCM from typical primary emission sources. No obvious UCM humps were found in total ion chromatograms (TIC) of the PM$_{2.5}$ samples collected during July–October, while the determined UCM reached 6.51 ± 4.92 μg/m^3 at the urban site and 6.75 ± 4.78 μg/m^3 at the rural site during November–May, accounting for ~9% of PM$_{2.5}$ mass at both sites. The missing UCM humps in the hot months were due to much large fraction of these semi-volatiles partitioning to gas phase and their much faster atmospheric oxidation. In addition, the lower organic matter (OM) was also a non-negligible factor contributing to less particulate UCM in summer. Five major sources for PM$_{2.5}$-bound UCM were identified by positive matrix factorization (PMF) involving organic and inorganic molecular source tracers. Vehicle exhaust accounted for 44.4% and 30.3% of UCM at the urban and the rural site,

respectively. Biomass burning contributed more to UCM at the rural site (28.0%) than at the urban site (19.2%). Ship emission was found to contribute substantially to UCM (28.9% at the urban and 17.3% at the rural site) in the PRD harbor megacity. Coal combustion and dust altogether contributed much less at the urban site (7.5%) than at the rural site (24.4%).

1. Introduction

The unresolved complex mixtures (UCM), often appearing in total ion chromatograms (TIC) as raised baseline humps, mainly consists of many groups of aliphatic branched and cyclic hydrocarbon isomers that is unable to be separated by conventional gas chromatography (James et al., 1999; Robinson et al., 2007). The term UCM was first used by Farrington and Quinn (1973) to describe the unresolved portion in the extracts of Narragansett Bay sediments. Subsequently, a growing number of literatures reported UCM detected in sediments and atmospheric aerosol samples associated with petroleum pollution (Frysinger et al., 2003; Ventura et al., 2007; Rogge et al., 2012; Chan et al., 2013; Nallathamby et al., 2014). However, some studies have pointed out that biomass burning also contributed to the UCM in aerosols (Rogge et al., 1998; Hays et al., 2004; Schmidl et al., 2008).

Recently, there are new concerns about semi-volatile UCM as important precursors of secondary organic aerosol (SOA) (Robinson et al., 2007; Zhao et al., 2014). Traditionally, SOA has long been considered to be formed by complex atmospheric oxidation of biogenic and anthropogenic volatile organic compounds (Odum et al., 1997a,b; Claeys et al., 2004; Cai and Griffin, 2006; Kiendlerscharr et al., 2009; Deng et al., 2017). But recent chamber studies reported that SOA production cannot be completely explained by these traditionally found VOCs, suggesting that unknown SOA precursors that are not included in their studies may in part fill this gap (Weitkamp et al., 2007; Deng et al., 2017; Liu et al., 2017). Robinson et al. (2007) proposed that semi-volatile organic compounds (SVOCs), as a source of the missing SOA precursors, should be partly responsible for discrepancies between field observations and model predictions of SOA. SVOCs, defined as a class of organics that have effective saturation concentration between 0.1 and 1000 $\mu g/m^3$, can partition between gas and particle phase depending on environmental conditions (Robinson et al., 2007; Chan et al., 2016). They have higher SOA yields compared to traditional VOCs, and models that include atmospheric chemistry of SVOCs tend to have an improved prediction of SOA loading in ambient air (Pye and Seinfeld, 2010; Jathar et al., 2014; Zhao et al., 2016). Therefore, oxidations of SVOCs are considered as an important source of SOA in ambient air (Hodzic et al., 2010; Woody et al., 2015). These SVOCs, however, could not be fully separated and identified by the traditional chromatography-mass spectrometry method, instead most of them appears as UCM in TIC. Chan et al. (2013) previously reported UCM can make up more than 80% SVOCs emitted by vehicle exhaust, therefore it might be an important source contributing to SOA formation especially in urban areas.

Although it is almost impossible for a large number of complex constitutes in UCM band to be completely identified and quantified, estimation of the bulk UCM may help to achieve mass balance closure. However, till now even ambient levels of atmospheric UCM are rarely reported. Previous studies reported the concentration of atmospheric UCM could reach more than 1 $\mu g/m^3$, accounting for large fractions of detected organic matter in aerosol (Tsapakis et al., 2002; Bi et al., 2008). Moreover, UCM has been considered as fingerprint of petroleum pollution (Frysinger et al., 2003; Rogge et al., 2012; Chan et al., 2013), but some researchers also found UCM in TIC of biomass burning aerosol samples (Hays et al., 2004). Until now, no quantifiable results of source contributions for UCM in field air environment are reported. In this study, ambient PM$_{2.5}$-bound UCM in the Pearl River Delta (PRD) region were characterized based on field samples collected at an urban site and a rural site in order to estimate the ambient levels, seasonal variations,

hump shapes and source contributions of PM$_{2.5}$-bound UCM.

2. Experimental sections

2.1. Field sampling

Fig. 1 shows the geographical locations of two sampling sites. Both sites are ambient air quality monitoring stations operated by local environmental monitoring centers. Urban SZ (23.13°N,113.27°E) is located in the city center with heavy traffic and dense population while rural JL (23.30°N, 113.57°E) in the northeast of Guangzhou is surrounded by large area of forest. More detailed information about sampling sites can be found elsewhere (Yu et al., 2017). A high volume sampler (Tisch Environmental, Inc., Ohio, USA) was used to collect PM$_{2.5}$ samples at a flow rate of 1.1 m^3/min with a quartz fiber filter (8 inch × 10 inch, Whatman, America). Meanwhile, Teflon filters (47 mm in diameter, Whatman, USA) samples were also collected by a medium-volume sampler with a flow rate of 16.7L/min (Model PQ-200, BGI Inc., USA) to analyze heavy metal elements. 24-h PM$_{2.5}$ sampling was conducted every five days from 23 July 2013 to 29 May 2014 at JL and from 26 August 2013 to 29 April 2014 at SZ to characterize PM$_{2.5}$-bound UCM. Moreover, PM$_{2.5}$ samples were extensively collected every day in August, November and December to capture typical pollution processes. In total, 101 and 84 PM$_{2.5}$ filter samples were collected at JL and SZ, respectively. Prior to sampling, the quartz fiber filter was pre-baked at 450 °C for 8 h to eliminate any adsorbed organics. Field and laboratory blanks were collected and analyzed in the same manner as the PM$_{2.5}$ samples during the whole experiment process. As shown in Fig. S1, all target compounds and UCM hump were not found or presented negligible level in blanks.

In order to characterize the particulate UCM emitted by on-road vehicles and ships, tunnel PM$_{2.5}$ samples and particulates in ship exhaust were also collected. The detailed sampling information can be found elsewhere (Zhang et al., 2015; Huang et al., 2017; Wu et al., 2019).

2.2. Laboratory analysis

2.2.1. Sample preparation

The more detailed description of sample preparation can be found elsewhere (Yu et al., 2017). Briefly, 1/4 of the sampled quartz fiber filter was spiked with internal standards including n-hexadecane-D$_{24}$, n-tetracosane-D$_{50}$, n-triacontane-D$_{62}$ and levoglucosan-^{13}C$_6$ and was firstly ultrasonically extracted twice with 30 mL mixed solvent of Dichloromethane (DCM)/Hexane (1:1, v:v), and then twice with the 30 mL mixed solvent of Dichloromethane/Methanol (1:1, v:v). The extracts from the four-time ultrasonic extractions were combined, filtered, and concentrated to ~1 mL, which was further separated into two parts. One part for methylation was blown to dryness under a gentle nitrogen and added with 200 μL of DCM, 10 μL of Methanol, and 300 μL of freshly prepared diazomethane. The methylated extracts were used to analyze normal alkanes (n-alkanes), polycyclic aromatic hydrocarbons (PAHs), organic acids and hopanes. The other part for silylation was blown to dryness and added with 100 μL of pyridine and 200 μL of N, O-bis-(trimethylsilyl)-trifluoroacetamide plus 1% trimethylchlorosilane at 70 °C for 1 h. The silylated extracts were used for analyzing biomass burning tracer, levoglucosan.

2.2.2. Determining organic compounds by gas chromatography-mass spectrometry

A gas chromatography/mass spectrometer detector (Agilent, 7890 GC/5975 MS) with a capillary column (Agilent HP-5 MS, 30 m × 0.25 mm × 0.25 μm) was employed to analyze the prepared samples. 1 μL of each sample was injected in splitless mode at a constant flow rate of high purity helium (1.2 mLmin^{-1}). The GC initial temperature was 65 °C, held for 2 min, then increased to 290 °C at 5 °C min^{-1} and kept for 20 min. N-alkanes, hopanes, PAHs and levoglucosan were identified based on their retention times and fragment ions, and then quantified against the corresponding calibration curves with authentic standards.

2.2.3. Organic carbon (OC) and elemental carbon (EC) analysis

A punch of quartz filter with an area of 1.5 cm^2 was taken to determine the concentration of OC and EC using the thermo-optical transmittance (TOT) method (NIOSH, 1999) by an OC/EC analyzer (Sunset Laboratory Inc., USA).

2.3. Heavy metal elements analysis

Each Teflon filter with area of 5.06 cm^2 was used for the analysis of heavy metals. The elements were microwave digested with 5 mL HNO$_3$ and 2 mL HF under the conditions of high temperature and high pressure (Tao et al., 2014). After cooling, a heating apparatus (120 °C) was used to reduce the acidity of extracted solution. 17 elements (Na, K, Ca, Mg, Al, Fe, Zn, Pb, Mn, Ti, V, Cr, Ni and Cu) were determined by ICP-MS (Thermo, USA).

2.4. Gas/particle partitioning of n-alkanes

Because volatility of n-alkanes varies systematically with carbon number (Presto et al., 2012) and they were detected across the entire UCM band, n-alkanes were used as surrogates to evaluate the gas/particle partitioning of UCMs. With the particulate phase concentration of n-alkanes determined as described above in section 2.2, concentrations of gas-phase n-alkanes were calculated based on the gas/particle partitioning theory by Pankow (1994), as below:

$$K_{p,OM} = \frac{K_p}{f_{OM}} = \frac{F/M_{OM}}{A} \tag{1}$$

$$K_{p,OM} = \frac{RT}{10^6 MW_{OM}\xi_{OM}P_L^0} \tag{2}$$

$$P_L^0 = P_L^{0,*} exp\left[\frac{\Delta H_{vap}^*}{R}\left(\frac{1}{298.15} - \frac{1}{T}\right)\right] \tag{3}$$

where particulate organic matter (OM) is assumed to be responsible for the absorptive uptake. K_p (m^3/μg) is the G/P partitioning coefficient and f_{OM} is the mass fraction of absorbing OM phase in total PM phase. F and A are the concentration (ng/m^3) of each n-alkane in particle phase and gas phase, respectively. M_{OM} (μg/m^3) is mass concentration of OM in particle phase. In eq (2), R (8.206 × 10^{-5} m^3 atm mol^{-1}K^{-1}) is the ideal gas constant and T (K) is ambient temperature. MW_{OM} (g/mol) is the average molecular weight of the absorptive OM phase. ξ_{OM} is the activity coefficient of each compound absorbed in OM phase and P_L^0 (atm) is the vapor pressure of each pure compound. In eq (2), P$^{0,*}_L$ (atm) is the vapor pressure of each pure compound at 298.15 K ΔH^*_{vap} (kJ/mol) is the enthalpy of vaporization of the liquid at 298.15 K. The value of f_{OM}, MW_{OM}, P$^{0,*}_L$ and ΔH^*_{vap} were taken from Xie et al. (2013, 2014). The values of F for each n-alkanes in this study were obtained from filter-based PM$_{2.5}$ measurement. The M_{OM} was estimated by multiplying the measured OC concentrations by a scaling factor of 2 (Chen and Yu, 2007; Gao et al., 2015). The meteorological data including ambient temperature and solar radiation were monitored during the sampling campaign (Table S2).
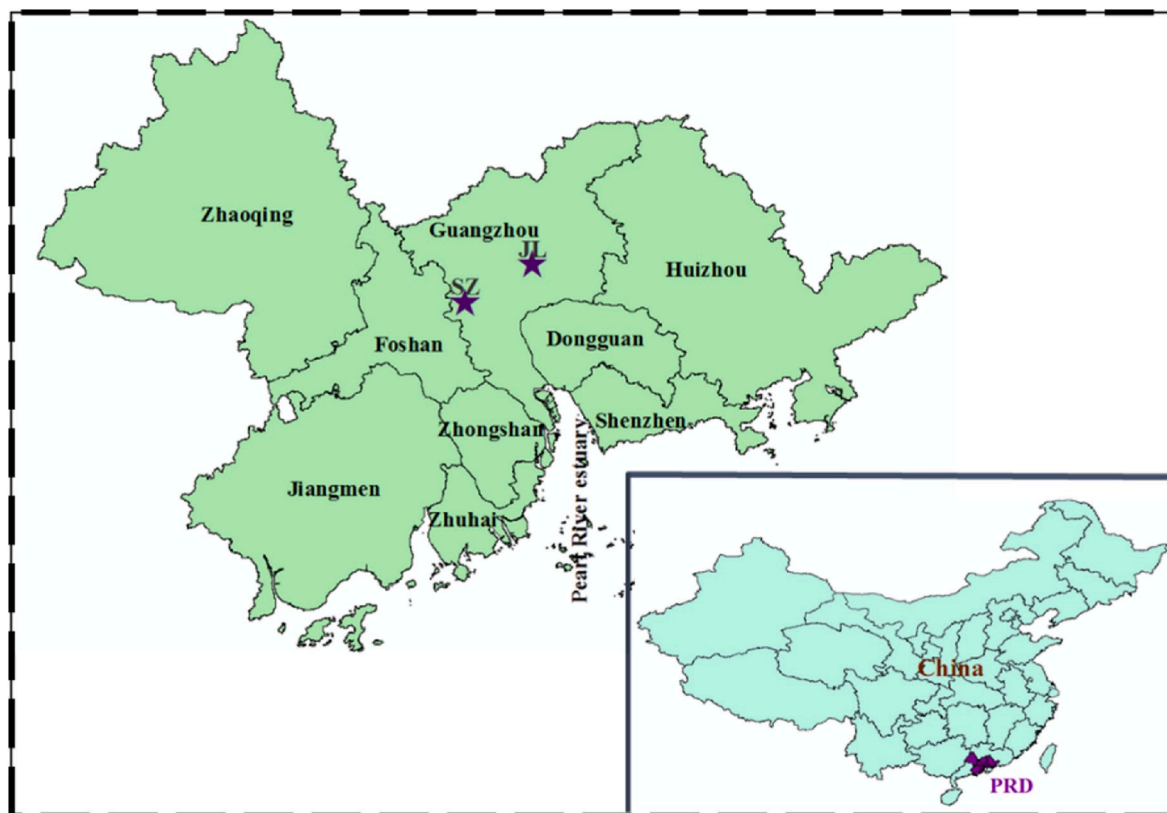

Fig. 1. Location of two sampling sites (PRD: the Pearl River Delta region in China).

2.5. Quantifying PM$_{2.5}$-bound UCM

As shown in Fig. 2, UCM was a large hump that mainly consisted of branched and cyclic alkanes (Fraser et al., 1997; Schauer et al., 2002; Tkacik et al., 2012). Actually, the oxidations, like acids, do not appear as a hump in TIC. Fig. S3 displayed the chromatogram of methylated fatty acids in a sample with UCM, we can see that these acid, though some of which had very high response in GC, did not form a hump in TIC. In addition, based on mass spectrum of UCM, m/z 57, 71 and 85 (typically aliphatic alkanes) and/or m/z 55, 69, 83 and 97 (typically cyclic alkanes) were major ions demonstrated in the UCM range (Fig. S4), implying that they are largely primary hydrocarbons, consistent with previous studies (Chan et al., 2013; Nallathamby et al., 2014). Because n-alkane homologues were detected across UCM band range, they have been used as alternative standards for quantifying level of UCM in environment samples (Phuleria et al., 2006; Wang et al., 2012b; Nallathamby et al., 2014; Zhao et al., 2014). In this study, the mass of PM$_{2.5}$-bound UCM is calculated using the approach outlined in Doskey (2001), which is briefly introduced here. UCM hump areas are determined by subtracting the total area of all peaks and a blank-solvent chromatogram from the total area obtained by integrating a sample chromatogram along the baseline, and then the average response factor of respective n-alkanes (C$_{14}$–C$_{36}$) in co-eluting UCM band was applied to determine the levels of PM$_{2.5}$-bound UCM (Doskey, 2001; Št'ávová at al., 2012). The detailed information of quantifying n-alkanes and UCM is provided in supporting information.

2.6. Positive matrix factorization (PMF)

USEPA PMF version 5.0 was employed in this study to resolve source contributions of measured UCM. The method is described in greater detail elsewhere (Paatero and Tapper, 1994; Paatero, 1997; Paterson et al., 1999). Briefly, data values below the method detection limits (MDLs) were substituted with MDL/2. The median concentrations were used for missing data values. If the concentration is less than or equal to the MDL used, the uncertainty is calculated using the equation of $Unc = 5/6 \times MDL$. If the concentration is greater than MDL used, the uncertainty is calculated by $Unc = [(Error\ Fraction \times concentration)^2 + (0.5 \times MDL)^2]^{1/2}$.

2.7. Backward trajectory analysis

The transporting paths of air masses during the campaign were investigated by Hybrid Single-Particle Lagrangian Integrated Trajectory model (HYSPLIT 4.0), which was developed by the National Oceanic and Atmospheric Administration (NOAA) (http://www.arl.noaa.gov/ready/hysplit4.html). The model was run every 1 h and the cluster analysis was performed in Fig. S7, which was based on 48-h backward air trajectories with starting height at 500 m.

3. Results and discussion

3.1. The concentrations of PM$_{2.5}$-bound UCM

No obvious UCM humps were found in TICs for PM$_{2.5}$ samples collected from July to October (Fig. 4). An explanation for missing UCM in these samples collected in the hot months is presented in section 3.2. In the other months (from November 2013 to May 2014), however, the average concentrations of determined PM$_{2.5}$-bound UCM at urban SZ and rural JL were 6.51 ± 4.92 μg/m^3 and 6.75 ± 4.78 μg/m^3, respectively. The UCM mass concentrations measured in this study were significantly higher than that measured in Guangzhou from June 2002 to July 2003 (1.6 μg/m^3 for annual average of UCM in TSP) (Bi et al., 2008), in Xiamen during the same months in 2015 (0.25–0.40 μg/m^3 for UCM in TSP) (Tao et al., 2017), in Santiago (0.84–1.37 μg/m^3 for UCM in PM$_{2.5}$ during the winter-spring season) (Tsapakis et al., 2002) and at nonurban sites in Europe (0.28 μg/m^3 for maximum concentration of PM$_{2.5}$-bound UCM in winter) (Oliveira et al., 2007). UCM on average accounted for $8.9 \pm 4.5\%$ and $9.2 \pm 6.4\%$ of PM$_{2.5}$ masses at SZ and JL, respectively. These percentages were comparable to but at the high-end of those reported in previous studies (2.2–11.8%) (Schauer et al., 1999; Hays et al., 2004).

Fig. 3 displays the temporal variation of UCM, PM$_{2.5}$ and EC at two sampling sites. At both sites estimated UCM concentrations presented consistent temporal variations with EC, which is a component solely from primary emission. This is reasonable since UCMs are largely from primary emissions. PM$_{2.5}$ and UCM, however, were not always positively correlated at the two sites as Fig. 3 demonstrated. This is also reasonable given that in ambient PM$_{2.5}$ about 50% or more are typically secondary inorganic and organic aerosols (Wang et al., 2012a; Huang et al., 2014). Nonetheless, as showed in Fig. 3, there were peak values of UCM corresponding to high PM$_{2.5}$ levels (such as samples collected on 16 March 2014 at SZ and on 12 December 2013 at JL), indicating that primary emission had a significant contribution to high PM$_{2.5}$ pollution events.

3.2. Missing UCM humps in hot months

As shown in Fig. 4, no obvious UCM hump was observed in TIC of PM$_{2.5}$ samples collected during July–October. As reported by Nallathamby et al. (2014), gas/particle partitioning could affect the collection
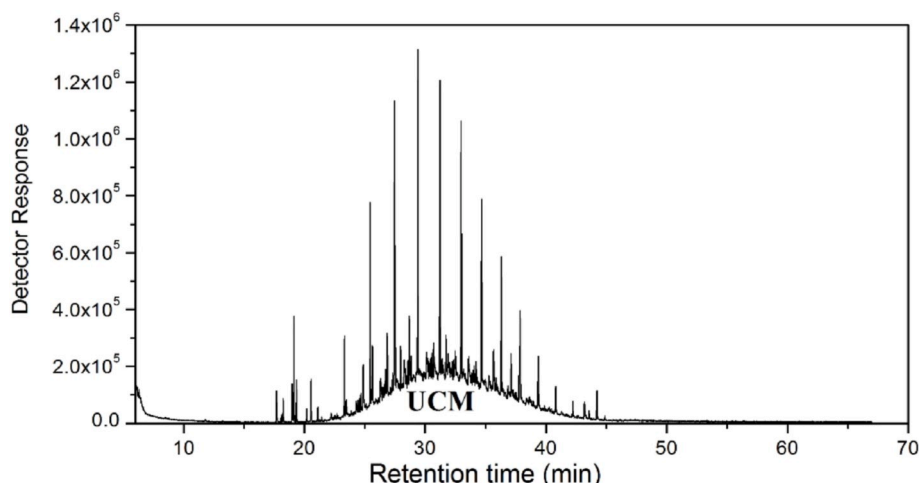
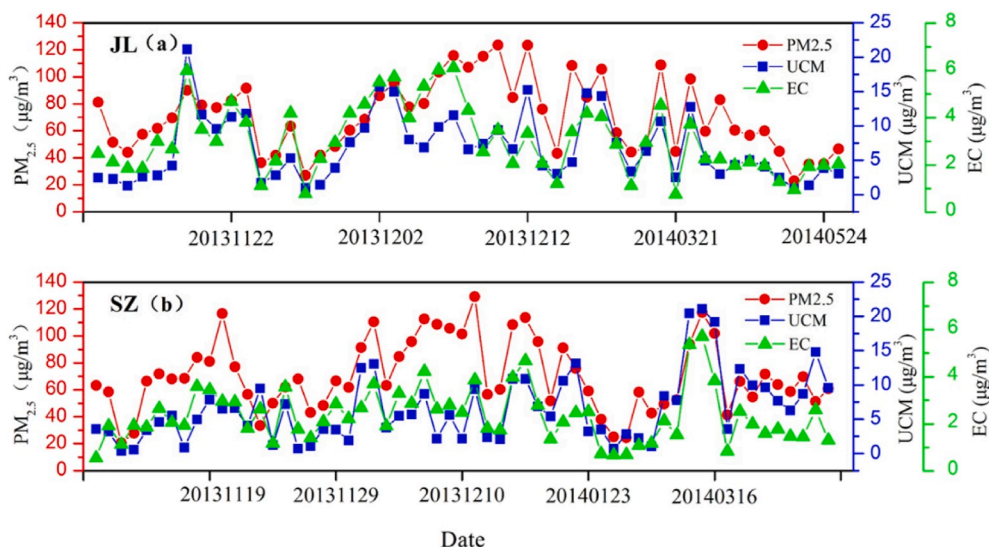**Fig. 2.** A diagram showing UCM in TIC.

Fig. 3. Temporal varation of $PM_{2.5}$, UCM and EC in SZ and JL from November 2013 to May 2014.
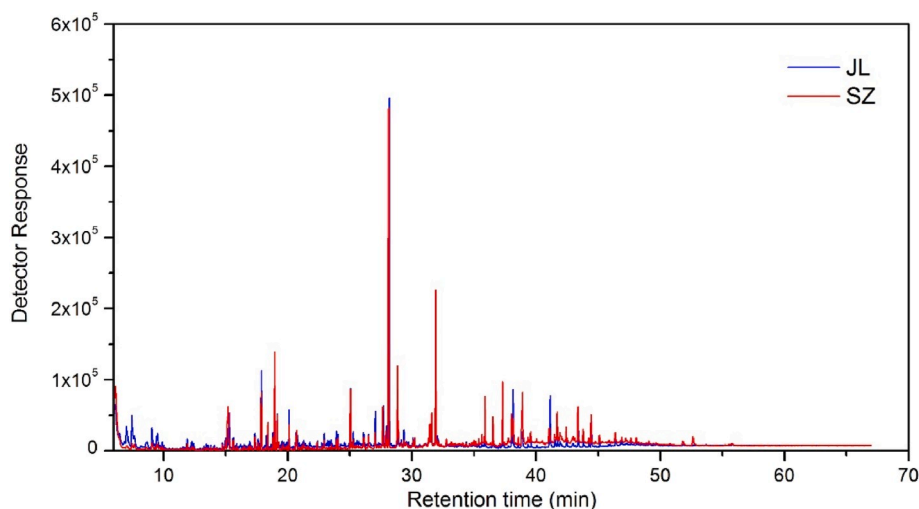

Fig. 4. Typical chromatograms of $PM_{2.5}$ samples of SZ and JL that collected in hot months (from July to October).

of particulate UCM and SVOCs tend to be partitioning into gas phase under higher ambient temperature. Tao et al. (2017) reported that the concentration of UCM in TSP samples was significantly higher in cold months (0.3 $\mu g/m^3$, the average value from November 2015 to April 2016) than that measured in hot months (0.1 $\mu g/m^3$, the average value from June to October, 2015) in Xiamen, China. As a matter of fact, this missing UCM during hot months were also reported by Simoneit et al. (1980) in the Lake Tahoe air basin or by Doskey and Andren (1986) in northern Wisconsin, where even the high-boiling UCM was barely detectable in particles collected during summer but was prominent in samples taken during winter. Although an explanation for the missing UCM in summer was not presented in previous studies, changes in source contributions should be excluded from the reasons for missing UCM in summer especially at the urban site SZ with heavy traffic in the neighborhood both in winter and in summer.

N-alkanes can be used as surrogates to evaluate the atmospheric process of UCM given that their volatility varies systematically with carbon number (Presto et al., 2012) and they were detected across the entire UCM band. Based on gas-particle partitioning theory, gaseous n-alkanes were estimated (Table S4) with their counterparts in the particulate phase. N-alkanes with relative lower carbon number ($<C_{20}$) mainly existed in gas phase while congeners $> C_{32}$ that were nearly in

particle phase. As semi-volatile compounds, the homologues between C_{20} and C_{32} partition between gas and particulate phase, and this partitioning is temperature dependent (Pankow, 1994). During July–October, the ambient air temperature was relatively higher, with an average of 28 $\pm$ 0.98 °C, in contrast with an average of 18 $\pm$ 3.64 °C during other months of sampling campaign (Table S1). The vapor phase concentrations of these n-alkanes were relatively higher during the period with high temperature, such as C_{21}, ~80% of which existed in gas phase during hot months while ~50% of which existed in gas phase for the other months (Table S4). UCMs falling in between C_{20} and C_{32} had the similar volatility with these n-alkanes, resulting in consistent gas/-particle partitioning behavior in ambient air. Therefore, substantial UCM compounds partitioned into gas phase during the period with high ambient temperature, which caused less collection of UCM based on quartz filters. Moreover, the sampling artifact was a common issue during the quartz filter sampling, resulting in absorption-induced positive bias or volatilization-induced negative bias. The volatilization and absorption processes are inherently coupled, making the artifacts unavoidable but extremely difficult to be corrected. The high temperature in summer would amplify the volatilization-induced artifacts during the 24-h collection, causing some UCM in quartz filter evaporating into gas phase. This might also reduce the UCM collected by quartz filters.

Wang et al. (2016) previously reported that the lower particle-phase concentrations of semi-volatile organic compounds in summer were partially caused by the lower mass concentration of organic matter (OM) though its effect was less important than temperature. Here, the individual effects of temperature and OM were also discussed by using the Pankow theory (Pankow, 1994). The measured particle-phase concentration of C_{24} n-alkane in JL in summer (OC = 14 μg/m^3, T = 28 °C) were used to recalculate the particulate concentrations of C_{24} n-alkane when decreasing the temperature or increasing the OM mass concentration individually. Retaining the same total concentration (particle-phase and gas-phase) of C_{24} n-alkane (4.2 ng/m^3, Table S4), particle-phase C_{24} n-alkane was recalculated under the constant OM (OC = 14 μg/m^3) while decreasing the temperature (T = 18 °C) and under the constant temperature (T = 28 °C) while increasing the OM mass concentration (OC = 16.4 μg/m^3), respectively. The calculated particle-phase C_{24} n-alkane concentration was 3.03 ng/m^3 (OC = 14 μg/m^3, T = 18 °C) and 1.43 ng/m^3 (OC = 16.4 μg/m^3, T = 28 °C), respectively. Obviously, the effect of temperature was significantly greater than OM, which was consistent with results reported by Xie et al. (2013) and Wang et al. (2016).

Secondary reactions might be another factor that affected UCM hump in TIC (Nallathamby et al., 2014). Miracolo et al. (2010) demonstrated that the photo-oxidation of semi-volatile fraction of UCM would result in removal of the semi-volatile UCM. During the sampling campaign, the solar radiation in hot months was significantly higher than the other months (Table S2). UCM mainly consists of branched alkanes and cycloalkanes. Compared with linear alkanes, these aliphatic hydrocarbons are much easier to react with oxidants, such as hydroxyl radical, in the atmosphere (Finlayson-Pitts and Pitts, 2000). These semi-volatile hydrocarbon species are mainly removed by hydroxyl radical (OH) in ambient air with lifetimes that can be calculated

$$\tau_{OH} = \frac{1}{K_{OH} \times [OH]} \tag{4}$$

where K_{OH} is the OH reaction rate constant (cm^3•molecule^{-1}•s^{-1}), obtaining from previous studies (Kwok and Atkinson, 1995; Zhao et al., 2014). [OH] is the concentration of OH in ambient air (molecule•cm^{-3}). Based on the empirical equation (Ehhalt and Rohrer, 2000), the concentration of OH during the sampling campaign was estimated. The concentration of OH in hot months was significantly higher than in other months (Table S2). Since UCM consists of a large number of complex mixtures without known rate constants for reacting with •OH, here n-alkanes were used as surrogates to assess the fate of UCM in atmosphere and the rate constants K_{OH} for n-alkanes were obtained from previous studies (Kwok and Atkinson, 1995; Zhao et al., 2014). Average concentration of OH in hot months and other months were used to estimate atmospheric lifetime of n-alkanes in UCM band by using equation (4). During the hot months, as Table S5 presented, the atmospheric lifetime of n-alkanes was significantly reduced with the enhancement of OH concentration, close to half of that estimated in other months. Therefore, gaseous UCMs were consumed at significantly higher rates under the high OH concentrations during hot months, which could interfere with the gas/particle distribution equilibrium and enable more particulate UCMs to partition into vapor phase. This atmospheric process significantly reduced atmospheric UCMs collected by quartz filters (Fig. S2). However, the oxidation products from UCM were less addressed in previous studies. As atmospheric UCM and the oxidation products are very complex and currently we even lack robust techniques to distinguish whether the oxidation products were formed from UCM or other precursors. Therefore, advanced techniques is needed to be developed in the future for resolving the UCM species and for characterizing their oxidation products.

To sum up, more particulate UCMs partitioning into vapor phase and much stronger photo-oxidation of gaseous UCMs were important factors that caused no obvious UCM hump in TIC of filter samples collected in the hot months. Meanwhile the lower organic matter in summer was also a non-negligible factor causing less UCM in aerosol phase though its effect was less significant than temperature effect.

3.3. Characterization of the UCM hump in TIC

Previous studies have reported that the appearance of sediment UCM hump that presented in TIC was related with initial sources (Ventura et al., 2007, 2008). Jeon et al. (2017) used the shape of UCM in TIC as an indicator to distinguish soils contaminated by different oil types. Nallathamby et al. (2014) reported that UCM was characterized with bimodal, UCM-A and UCM-B in PM$_{2.5}$ samples of Bakersfield. The UCM-A, consisting of compounds with lower carbon numbers, was from diesel emissions while the heavier UCM-B with the similar pattern to the samples containing crude oil or motor oil pollution was considered as urban source contributions including traffic. In this study, three types of source samples, including dust samples, tunnel samples and ship exhaust samples, were used to help characterize the UCM hump. The dust samples were NIST Standard Reference Material (SRM 1649b). 42 tunnel samples and 11 ship exhaust samples of were collected in Guangzhou (Zhang et al., 2015; Huang et al., 2017; Wu et al., 2019). Typical TICs for these sources are displayed in Fig. 5. Because the combustion of gasoline (<C12) and diesel oil (C12–C22) do not contribute these high weight molecular organics around n-C_{29} or n-C_{30}, the late-eluting UCMs were attributed to emissions from the motor oil combustion (Zhao et al., 2015, 2016; Alam et al., 2019). The retention time of UCM seemed to be vary to source types. The UCM presented in TIC of dust sample was similar to tunnel sample, representing vehicle emission, with UCM hump peak corresponding to high carbon number n-alkanes like n-C_{29} or n-C_{30}. While UCM in TIC of biomass burning sample centered from n-C_{22} to n-C_{24} (Schmidl et al., 2008). Furthermore, bimodal UCMs were found in TIC of ship exhaust samples. The peak of fore-eluting UCM ranged from n-C_{18} to n-C_{20} while the late-eluting UCM centered at n-C_{27} or n-C_{28}. This kind of UCM is similar to the one reported by Nallathamby et al. (2014). Heavy diesel oil was commonly used as fuel for ships, which could contribute the fore-eluting UCM (Miracolo et al., 2010). Generally, it can be indicated that diesel oil combustion and biomass burning could have contributed to fore-eluting UCM while motor oil combustion could be a significant source of late-eluting UCM. In addition, UCM humps in our ambient PM$_{2.5}$ samples were also characterized. As Fig. 6 displayed, UCM in Fig. 6a was characterized with two obvious peak, similar to the UCM reported by Nallathamby et al. (2014). Fig. 6b shows the unimodal UCM with late-eluting hump, which resembled the UCM features of dust and tunnel samples. The UCM hump presented in Fig. 6c was somewhat similar to ship exhaust samples, both had a wide UCM band. Moreover, no significant differences in the UCM retention time ranges between the two sampling sites were observed. This might be related to their source contributions. As indicated by source apportionment results in section 3.4, vehicle exhaust, which contributed to the late-eluting UCM, was dominant source of UCM at both sites. Ship emission and biomass burning, which contributed to the fore-eluting UCM, were both among the top three sources at the two sites, only that biomass burning ranked the second at the rural site while ship emission ranked the second at the urban site.

3.4. Source apportionment of PM$_{2.5}$-bound UCM

Early studies found UCM presented in fossil fuel products or that UCM contained in environmental samples was associated with petroleum pollution (Killops and Al Juboori, 1990; Gough and Rowland, 1990; Hildemann et al., 1991). Subsequently, extensive researches developed UCM hump as an environmental fingerprint to identify the samples affected by fossil fuel (Frysinger et al., 2003; White et al., 2013). However, other studies proposed that biomass burning also contributed to UCM in atmospheric aerosols (Oros and Simoneit, 2001; Hays et al., 2004; Schmidl et al., 2008). To further investigate the contribution of
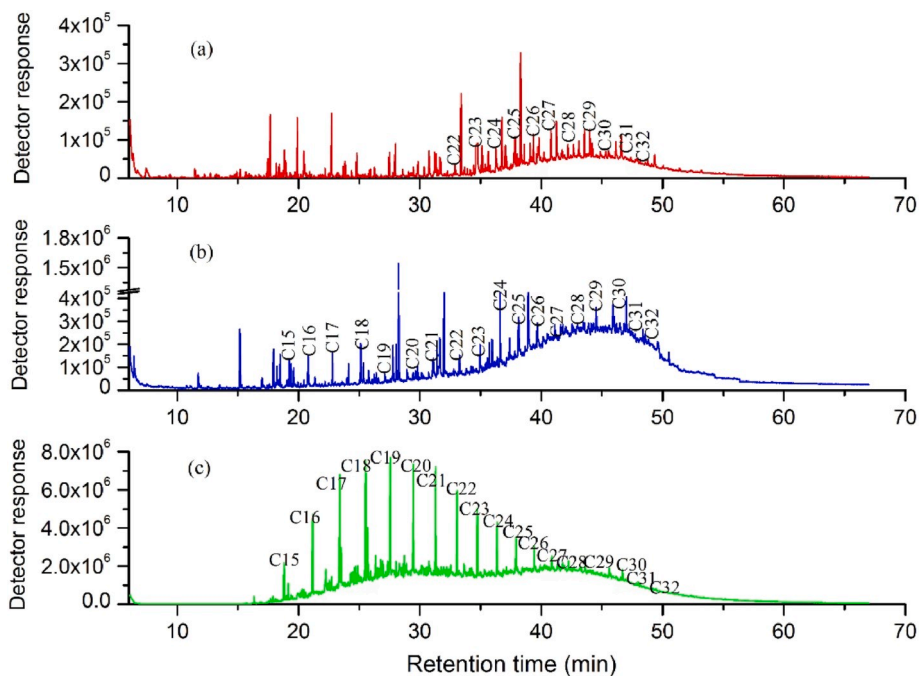
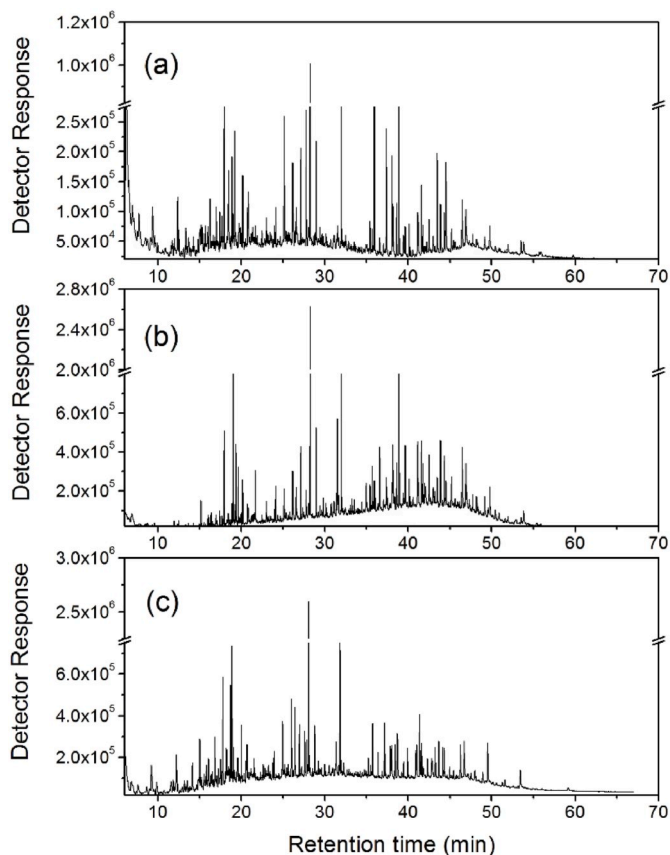**Fig. 5.** TIC of urban dust (a), tunnel sample (b) and ship exhaust (c).

Fig. 6. Typical chromatograms showing different types of UCM among PM$_{2.5}$ samples collected at two sampling sites: (a) sample collected on December 8, 2013 at JL; (b) sample collected December 12, 2013 at SZ; and (c) sample collected on March 11, 2014 at JL.
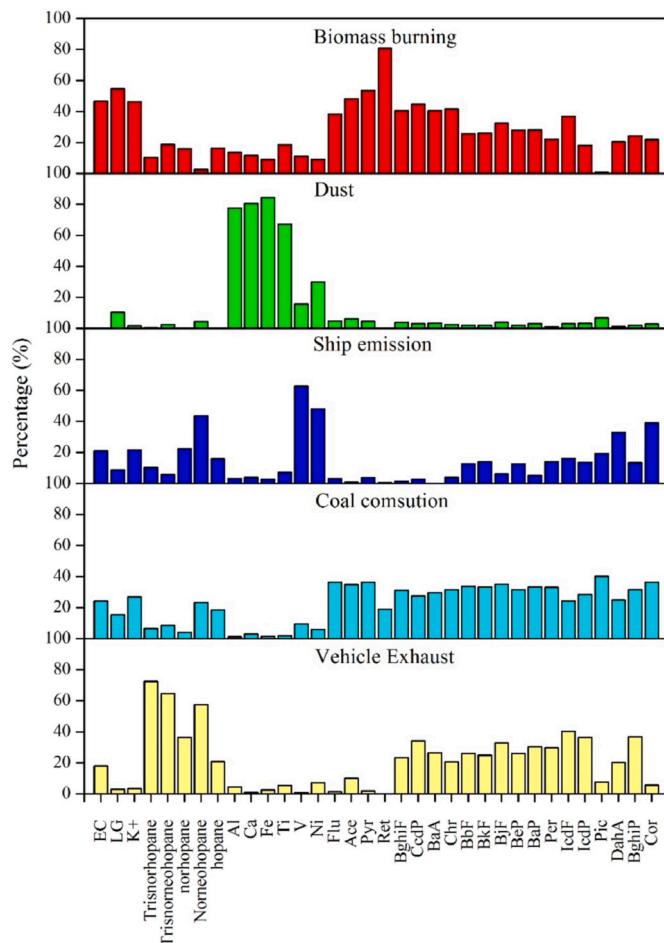

Fig. 7. Sources profiles (% of the species) resolved by the PMF model.

different emission sources to ambient $PM_{2.5}$-bound UCM, positive matrix factorization (PMF) model was used in this study. 35 species including UCM, EC, levoglucosan (LG), K^+, 5 hopanes, 6 heavy metal elements and 20 individual PAHs were input into the model. Finally, five sources were identified and their profiles were presented in Fig. 7. The first source was dominated by retene, LG and K^+, considering as contribution of biomass burning (Ramdahl, 1983; van Drooge and Ballesta, 2009). The second source with high percentage of crustal elements including Al, Ca, Fe, and Ti was considered as dust (Tao et al., 2014). The third source is characterized by high loading of V and Ni, which are related with emission from crude oil and are suggestive of ship emission (Zhang et al., 2013). The fourth source was identified as coal combustion by a significant presence of its marker picene and other PAHs with high molecular weight (Oros and Simoneit, 2001; Zhang et al., 2008). The fifth source, vehicle exhaust, is characterized by high contribution of hopanes, which is widely used as primary organic tracers of vehicle emission (Jaeckels et al., 2007; Ravindra et al., 2008; Wang et al., 2016).

The predicted and measured UCM showed significant correlation (R^2 = 0.82) with a slope of 0.89 (Fig. S5), suggesting that the resolved factors could explain the main sources of $PM_{2.5}$-bound UCM in the PRD. As displayed in Fig. 8, vehicle exhaust was a dominant source for $PM_{2.5}$-bound UCM at two sites, accounting for 44.4% and 30.3% at SZ and JL, respectively. Biomass burning was another important source at rural JL, contributing 28.0% of measured UCM to this site. However, this source had relatively lower contribution at the urban site, accounting for 19.2% UCM at SZ. It is worth noting that at both sites, ship emission contributed substantially to $PM_{2.5}$-bound UCM, especially at urban SZ with a share of 28.9% of measured UCM. A ratio of V/Ni higher than 0.7 was commonly used as an indicator for ship emission (Isakson et al., 2001; Viana et al., 2009). In this study, average ratios of V/Ni at SZ and JL were 3.02 and 2.95 (Fig. S6), respectively. These ratios were significantly higher than those calculated in $PM_{2.5}$ samples collected at Tuoji Island in Bohai Rim (V/Ni = 1.54), a region significantly influenced by ship emissions (Zhang et al., 2013). A high ratio of V/Ni in our $PM_{2.5}$ samples and UCM hump in the TIC of ship exhaust samples provided strong evidence that ship emission was a significant source for UCM in the PRD region. Dust accounted for 15.3% UCM at JL while this source only contributed 2.3% UCM at SZ. Coal combustion contributed a minor part of UCM at both two sites (5.2% at SZ, 9.1% at JL).

In addition, as demonstrated in Fig. S8, contributions to UCM by biomass burning and ship emission showed substantial monthly variation at the two sampling sites. Biomass burning contributed much more during November 2013–January 2014 than during February–April 2014. This is consistent with the significantly reduced LG (tracer for biomass burning) concentrations and the LG/OC ratios from January 2014 to April 2014 (Fig. S9). Contrarily, ship emission contributed less during November 2013–January 2014 than during February–April 2014 when more oceanic air masses, as depicted by backward trajectories (Fig. S7), would bring more ship emission to the sampling sites.

Given that semi-volatile UCM are a substantial part of organic matters in $PM_{2.5}$ and they play an important role in SOA formation, the source apportionment results implicated that to reduce the particulate UCM, stricter control measures are needed on vehicle (mainly diesel) emissions, which are previously regarded the major sources of UCM. Apart from vehicle emission, biomass burning is still a significant source for $PM_{2.5}$-bound UCM especially at the rural site, although regulations have been implemented by the Chinese governments to prohibit open burning of crops (Yan et al., 2006; Zhang et al., 2013). Our study also reveals that ship emission might be a very important source of UCM in harbor cities like Guangzhou.

4. Conclusions

$PM_{2.5}$ samples were collected at two sites (one rural site and one urban site) to investigate the $PM_{2.5}$-bound UCM. A semi-quantitative method was applied to estimate the ambient levels of the $PM_{2.5}$-bound UCM. No obvious UCM hump was found in TIC of $PM_{2.5}$ samples that collected from July to October since UCM SVOCs prefer partitioning into vapor phase and also they have much higher photo-oxidation rates in these hot months. Moreover, the lower organic matter in summer was also a non-negligible factor decreasing UCM in aerosol phase. The determined UCM mass concentration at urban SZ and rural JL were **6.51 ± 4.92 μg/m³ and 6.75 ± 4.78 μg/m³,** accounting for **8.9 ± 4.5%** and **9.2 ± 6.4%** of $PM_{2.5}$ mass, **respectively.**

Apart from comparing the $PM_{2.5}$-bound UCM humps with the UCM humps for the dust, tunnel, ship exhaust and biomass burning samples to indicate sources of UCM, PMF involving typical organic and inorganic tracers in $PM_{2.5}$ was applied for source apportionment of UCM. Vehicle emission contributed most to the $PM_{2.5}$-bound UCM at both sites, accounting for **44.4%** at SZ **and 30.3%** at JL. Biomass burning was also a significant source of UCM at rural JL with a share of 28.0%. Ship emission, to our surprise, had substantial contributions to $PM_{2.5}$-bound UCM with shares of 28.9% at urban SZ and 17.3% at rural JL. Dust accounted for 15.3% of UCM at rural JL but only a minor fraction at urban SZ (2.3%). Coal combustion contributed <10% of UCM, with a higher percentage at rural JL (9.1%) than urban SZ (5.2%).

Sources and atmospheric processes of UCM are very complex in ambient environment, and in the future advanced techniques such as two-dimensional gas chromatography coupled with time-of-flight mass spectrometry (GCXGC-TOF-MS) (Alam et al., 2019) can be applied to improve the characterization of UCM for better understanding of their chemical compositions, atmospheric abundances, emission sources and
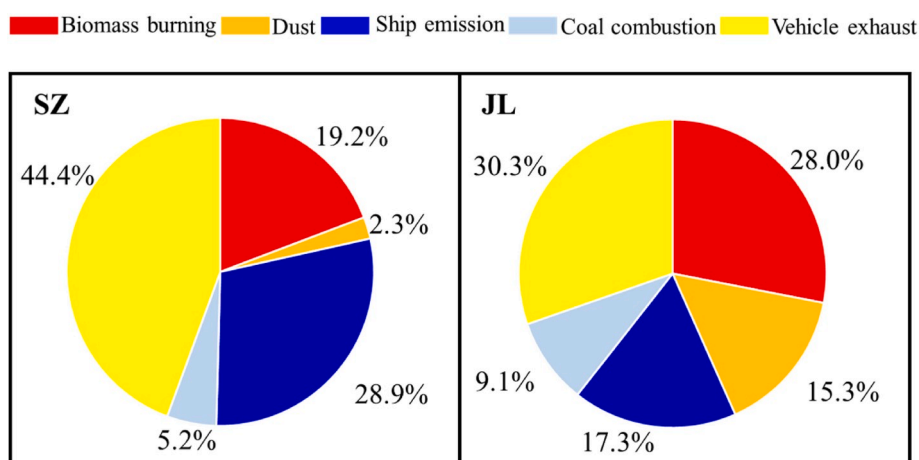

Fig. 8. Contributions of identified sources to measured UCM at the two sampling site.

atmospheric processing.

Declaration of competing interest

The authors declare that they have no known competing financial interests or personal relationships that could have appeared to influence the work reported in this paper.

CRediT authorship contribution statement

Hua Fang: Data curation, Formal analysis, Investigation, Methodology, Writing - original draft. **Scott D. Lowther:** Data curation, Formal analysis, Investigation. **Ming Zhu:** Data curation, Formal analysis, Methodology. **Chenglei Pei:** Data curation, Investigation. **Sheng Li:** Data curation, Investigation. **Zheng Fang:** Data curation, Investigation. **Xu Yu:** Data curation, Methodology. **Qingqing Yu:** Data curation, Methodology. **Yujun Wang:** Investigation. **Yanli Zhang:** Data curation, Investigation. **Kevin C. Jones:** Data curation, Methodology. **Xinming Wang:** Conceptualization, Data curation, Methodology, Funding acquisition, Supervision, Writing - review & editing.

Acknowledgments

Appendix A. Supplementary data

Supplementary data to this article can be found online at https://doi.org/10.1016/j.atmosenv.2020.117407.

References

Alam, M., Zeraati-Rezaei, S., Xu, H., Harrison, R., 2019. Characterization of gas and particulate phase organic emissions (C9–C37) from a diesel engine and the effect of abatement devices. Environ. Sci. Technol. 53, 11345–11352. https://doi.org/10.1021/acs.est.9b03053.

Bi, X., Simoneit, B.R.T., Sheng, G., Ma, S., Fu, J., 2008. Composition and major sources of organic compounds in urban aerosols. Atmos. Res. 88, 256–265. https://doi.org/10.1016/j.atmosenv.2014.07.056.

Cai, X.Y., Griffin, R.J., 2006. Secondary aerosol formation from the oxidation of biogenic hydrocarbons by chlorine atoms. J. Geophys. Res. 111, D14206. https://doi.org/10.1029/2005jd006857.

Chan, A.W.H., Isaacman, G., Wilson, K.R., Worton, D.R., Ruehl, C.R., Nah, T., Gentner, D. R., Dallmann, T.R., Kirchstetter, T.W., Harley, R.A., 2013. Detailed chemical characterization of unresolved complex mixtures in atmospheric organics: insights into emission sources, atmospheric processing, and secondary organic aerosol formation. J. Geophys. Res. 118, 6783–6796. https://doi.org/10.1002/jgrd.50533.

Chan, A.W.H., Kreisberg, N.M., Hohaus, T., Campuzano-Jost, P., Zhao, Y., Day, D.A., Kaser, L., Karl, T., Hansel, A., Teng, A.P., Ruehl, C.R., Sueper, D.T., Jayne, J.T., Worsnop, D.R., Jimenez, J.L., Hering, S.V., Goldstein, A.H., 2016. Speciated measurements of semivolatile and intermediate volatility organic compounds (S/ IVOCs) in a pine forest during BEACHON-RoMBAS 2011. Atmos. Chem. Phys. 16, 1187–1205. https://doi.org/10.5194/acp-16-1187-2016.

Chen, X., Yu, J.Z., 2007. Measurement of organic mass to organic carbon ratio in ambient aerosol samples using a gravimetric technique in combination with chemical analysis. Atmos. Environ. 41, 8857–8864. https://doi.org/10.1016/j.atmosenv.2007.08.023.

Claeys, M., Graham, B., Vas, G., Wang, W., Vermeylen, R., Pashynska, V., Cafmeyer, J., Guyon, P., Andreae, M.O., Artaxo, P., Maenhaut, W., 2004. Formation of secondary organic aerosols through photooxidation of isoprene. Science 303, 1173–1176. https://doi.org/10.1126/science.1092805.

Deng, W., Hu, Q., Liu, T., Wang, X., Zhang, Y., Song, W., Sun, Y., Bi, X., Yu, J., Yang, W., Huang, X., Zhang, Z., Huang, Z., He, Q., Mellouki, A., George, C., 2017. Primary particulate emissions and secondary organic aerosol (SOA) formation from idling diesel vehicle exhaust in China. Sci. Total Environ. 593–594, 462–469. https://doi.org/10.1016/j.scitotenv.2017.03.088.

Doskey, P.V., Andren, A.W., 1986. Particulate and vapor-phase n-alkanes in the northern Wisconsin atmosphere. Atmos. Environ. 20, 1735–1744. https://doi.org/10.1016/0004-6981(86)90122-8.Doskey.

Ehhalt, D.H., Rohrer, F., 2000. Dependence of the OH concentration on solar UV. J. Geophys. Res. Atmos. 105, 3565–3571. https://doi.org/10.1029/1999jd901070.

Farrington, J.W., Quinn, J.G., 1973. Petroleum hydrocarbons in Narragansett Bay: I. Survey of hydrocarbons in sediments and clams (Mercenaria mercenaria). Estuar. Coast Mar. Sci. 1, 71–79. https://doi.org/10.1016/0302-3524(73)90059-5.

Finlayson-Pitts, B.J., Pitts Jr., J.N., 2000. Chemistry of the upper and lower atmosphere: Theory, experiments, and applications. Academic Press, New York, p. 969. https://doi.org/10.1016/B978-0-12-257060-5.X5000-X.

Fraser, M.P., Cass, G.R., Simoneit, B.R.T., Rasmussen, R.A., 1997. Air quality model evaluation data for organics. 4. C_2-C_{36} nonaromatic hydrocarbons. Environ. Sci. Technol. 31, 2356–2367. https://doi.org/10.1021/es960980g.

Frysinger, G.S., Gaines, R.B., Xu, L., Reddy, C.M., 2003. Resolving the unresolved complex mixture in petroleum-contaminated sediments. Environ. Sci. Technol. 37, 1653–1662. https://doi.org/10.1021/es020742n.

Gao, B., Wang, X.M., Zhao, X.Y., Ding, X., Fu, X.X., Zhang, Y.L., He, Q.F., Zhang, Z., Liu, T.Y., Huang, Z.Z., Chen, L.G., Peng, Y., Guo, H., 2015. Source apportionment of atmospheric PAHs and their toxicity using PMF: impact of gas/particle partitioning. Atmos. Environ. 103, 114–120. https://doi.org/10.1016/j.atmosenv.2014.12.006.

Gough, M.A., Rowland, S.J., 1990. Characterization of unresolved complex mixtures of hydrocarbons in petroleum. Nature 344, 648–650. https://doi.org/10.1038/344648a0.

Hays, M.D., Smith, N.D., Dong, Y., 2004. Nature of unresolved complex mixture in size-distributed emissions from residential wood combustion as measured by thermal desorption-gas chromatographyemass spectrometry. J. Geophys. Res. Atmos. 109 (D16S04), 1–13. https://doi.org/10.1029/2003JD004051.

Hildemann, L.M., Mazurek, M.A., Cass, G.R., Simoneit, B.R.T., 1991. Quantitative characterization of urban sources of organic aerosol by high-resolution gas chromatography. Environ. Sci. Technol. 25, 1311–1325. https://doi.org/10.1021/es00019a014.

Hodzic, A., Jimenez, J.L., Madronich, S., Canagaratna, M.R., Decarlo, P.F., Kleinman, L., Fast, J., 2010. Modeling organic aerosols in a megacity: potential contribution of semi-volatile and intermediate volatility primary organic compounds to secondary organic aerosol formation. Atmos. Chem. Phys. 10, 5491–5514. https://doi.org/10.5194/acp-12-9025-2012.

Huang, R.J., Zhang, Y., Bozzetti, C., Ho, K.F., Cao, J.J., Han, Y., Daellenbach, K.R., Slowik, J.G., Platt, S.M., Canonaco, F., Zotter, P., Wolf, R., Pieber, S.M., Bruns, E.A., Crippa, M., Ciarelli, G., Piazzalunga, A., Schwikowski, M., Abbaszade, G., Schnelle-Kreis, J., Zimmermann, R., An, Z.S., Szidat, S., Baltensperger, U., Haddad, I.E., Prévôt, A.S., 2014. High secondary aerosol contribution to particulate pollution during haze events in China. Nature 514, 218–222. https://doi:10.1038/nature13774.

Huang, X.L., Zhang, Z., Yang, W.Q., Li, S., Zhu, M., Fang, H., He, J.J., Chen, J.W., Wan, C. H., Zhang, Y.L., Liu, G.G., Huang, Z.Z., Wang, J.Y., Wang, X.M., 2017. Emission Factors and Preliminary Emission Estimates of Air Pollutants from Ships at Berth in the Guangzhou Port. Huan Jing Ke Xue. https://doi.org/10.13227/j.hjkx.201612212.

Isakson, J., Persson, T.A., Lindgren, E.S., 2001. Identification and assessment of ship emissions and their effects in the harbour of Göteborg, Sweden. Atmos. Environ. 35, 3659–3666. https://doi.org/10.1016/S1352-2310(00)00528-8.

Jaeckels, J.M., Min-Suk, B., Schauer, J.J., 2007. Positive matrix factorization (PMF) analysis of molecular marker measurements to quantify the sources of organic aerosols. Environ. Sci. Technol. 41, 5763–5769. https://doi.org/10.1021/es062536b.

James, J.S., Michael, J.K., Glen, R.C., Bernd, R.T.S., 1999. Measurement of emissions from air pollution sources. 2. C1 through C30 organic compounds from medium duty diesel trucks. Environ. Sci. Technol. 33, 1578–1587. https://doi.org/10.1021/es980081n.

Jathar, S.H., Gordon, T.D., Hennigan, C.J., Pye, H.O.T., Pouliot, G., Adams, P.J., Donahue, N.M., Robinson, A.L., 2014. Unspeciated organic emissions from combustion sources and their influence on the secondary organic aerosol budget in the United States. Proc. Natl. Acad. Sci. Unit. States Am. 111, 10473–10478. https://doi.org/10.1073/pnas.1323740111.

Jeon, S.K., Kwon, D., Lee, S., 2017. Identification of weathered multiple petroleum products in contaminated soils by characterizing unresolved complex mixture hump in gas chromatogram data. Sci. Total Environ. 607–608, 42–52. https://doi.org/10.1016/j.scitotenv.2017.06.251.

Kiendlerscharr, A., Wildt, J., Maso, M.D., Hohaus, T., Kleist, E., Mentel, T.F., Tillmann, R., Uerlings, R., Schurr, U., Wahner, A., 2009. New particle formation in forests inhibited by isoprene emissions. Nature 461, 381. https://doi.org/10.1038/nature08292.

Killops, S.D., Al-Juboori, M.A.H.A., 1990. Characterisation of the unresolved complex mixture (UCM) in the gas chromatograms of biodegraded petroleums. Org. Geochem. 15, 147–160. https://doi.org/10.1016/0146-6380(90)90079-F.

Kwok, E.S.C., Atkinson, R., 1995. Estimation of hydroxyl radical reaction-rate constants for gas-phase organic-compounds using a structure-reactivity relationship - an update. Atmos. Environ. 29, 1685–1695. https://doi.org/10.1016/1352-2310(95)00069-B.

Liu, T., Li, Z., Chan, M.N., Chan, C.K., 2017. Formation of secondary organic aerosols from gas–phase emissions of heated cooking oils. Atmos. Chem. Phys. 17, 1–30. https://doi.org/10.5194/acp-17-7333-2017.

Miracolo, M.A., Presto, A.A., Lambe, A.T., Hennigan, C.J., Donahue, N.M., Kroll, J.H., Worsnop, D.R., Robinson, A.L., 2010. Photo-oxidation of low-volatility organics found in motor vehicle emissions: production and chemical evolution of organic

aerosol mass. Environ. Sci. Technol. 44, 1638–1643. https://doi.org/10.1021/es902635c.

Nallathamby, P.D., Lewandowski, M., Jaoui, M., Offenberg, J.H., Kleindienst, T.E., Rubitschun, C., Surratt, J.D., Usenko, S., Sheesley, R.J., 2014. Qualitative and quantitative assessment of unresolved complex mixture in PM $_{2.5}$ of Bakersfield, CA. Atmos. Environ. 98, 368–375. https://doi.org/10.1016/j.atmosenv.2014.09.006.

NIOSH, 1999. Method 5040 Issue 3: elemental carbon (diesel exhaust). In: NIOSH Manual of Analytical Methods. National Institute of Occupational Safety and Health, Cincinnati, OH.

Odum, J.R., Jungkamp, T.P.W., Griffin, R.J., Flagan, R.C., Seinfeld, J.H., 1997a. The atmospheric aerosol-forming potential of whole gasoline vapor. Science 276, 96–99. https://doi.org/10.1126/science.276.5309.96.

Odum, J.R., Jungkamp, T.P.W., Griffin, R.J., Forstner, H.J.L., Flagan, R.C., Seinfeld, J.H., 1997b. Aromatics, reformulated gasoline, and atmospheric organic aerosolformation. Environ. Sci. Technol. 31, 1890–1897. https://doi.org/10.1021/es960535l.

Oliveira, T.S., Pio, C.A., Alves, C.A., Silvestre, A.J.D., Evtyugina, M., Afonso, J.V., Fialho, P., Legrand, M., Puxbaum, H., Gelencsér, A., 2007. Seasonal variation of particulate lipophilic organic compounds at nonurban sites in Europe. J. Geophys. Res. Atmos. 112, 107–114. https://doi.org/10.1029/2007JD008504.

Oros, D.R., Simoneit, B.R.T., 2001. Identification and emission factors of molecular tracers in organic aerosols from biomass burning Part 2. Deciduous trees. Appl. Geochem. 16, 1545–1565. https://doi.org/10.0883-2927(01)00022-1.

Doskey, Paul V., 2001. Spatial variations and chronologies of aliphatic hydrocarbons in Lake Michigan Sediments. Environ. Sci. Technol. 35, 247–254. https://doi.org/10.1021/es001365m.

Paatero, P., 1997. Least squares formulation of robust non-negative factor analysis. Chemom. Intell. Lab. 37, 23–35. https://doi.org/10.1016/S0169-7439(96)00044-5.

Paatero, P., Tapper, U., 1994. Positive matrix factorization - a nonnegative factor model with optimal utilization of error-estimates of data values. Environmetrics 111–126. https://doi.org/10.1002/env.3170050203.

Pankow, J.F., 1994. An absorption model of gas/particle partitioning of organic compounds in the atmosphere. Atmos. Environ. 28, 185–188. https://doi.org/10.1016/1352-2310(94)90093-0.

Paterson, K.G., Sagady, J.L., Hooper, D.L., 1999. Analysis of air quality data using positive matrix factorization. Environ. Sci. Technol. 33, 635–641. https://doi.org/10.1021/Es980605j.

Phuleria, H.C., Geller, M.D., Fine, P.M., Sioutas, C., 2006. Size-resolved emissions of organic tracers from light- and heavy-duty vehicles measured in a California roadway tunnel. Environ. Sci. Technol. 40, 4109–4118. https://doi.org/10.1021/es052186d.

Presto, A.A., Hennigan, C.J., Nguyen, N.T., Robinson, A.L., 2012. Determination of volatility distributions of primary organic aerosol emissions from internal combustion engines using thermal desorption gas chromatography mass spectrometry. Aerosol Sci. Technol. 46, 1129–1139. https://doi.org/10.1080/02786826.2012.700430.

Pye, H.O.T., Seinfeld, J.H., 2010. A global perspective on aerosol from low-volatility organic compounds. Atmos. Chem. Phys. 10, 4377–4401. https://doi.org/10.5194/acp-10-4377-2010.

Ramdahl, T., 1983. Retene - a molecular marker of wood combustion in ambient air. Nature 306, 580e583. https://doi.org/10.1038/306580a0.

Ravindra, K., Sokhi, R., Grieken, R., 2008. Atmospheric polycyclic aromatic hydrocarbons: source attribution, emission factors and regulation. Atmos. Environ. 42, 2895–2921. http://dio.10.1016/j.atmosenv.2007.12.010.

Robinson, A.L., Donahue, N.M., Shrivastava, M.K., Weitkamp, E.A., Sage, A.M., Grieshop, A.P., Lane, T.E., Pierce, J.R., et al., 2007. Rethinking organic aerosols: semivolatile emissions and photochemical aging. Science 315, 1259–1262. https://doi.org/10.1126/science.1133061.

Rogge, W.F., Hildemann, L.M., Mazurek, M.A., Cass, G.R., Simoneit, B.R.T., 1998. Sources of fine organic aerosol. 9. Pine, oak, and synthetic log combustion in residential fireplaces. Environ. Sci. Technol. 32, 13–22. https://doi.org/10.1021/es960930b.

Rogge, W.F., Medeiros, P.M., Simoneit, B.R.T., 2012. Organic compounds in dust from rural and urban paved and unpaved roads taken during the San Joaquin Valley fugitive dust characterization study. Environ. Eng. Sci. 29, 1–13. https://doi.org/10.1089/ees.2010.0124.

Schauer, J.J., Kleeman, M.J., Cass, G.R., Simoneit, B.R.T., 1999. Measurement of emissions from air pollution sources. 2. C_1 through C_{30} organic compounds from medium duty diesel trucks. Environ. Sci. Technol. 33, 1578–1587. https://doi.org/10.1021/es980081n.

Schauer, J.J., Kleeman, M.J., Cass, G.R., Simoneit, B.R.T., 2002. Measurement of emissions from air pollution sources. 5. C_1-C_{32} organic compounds from gasoline-powered motor vehicles. Environ. Sci. Technol. 36, 1169–1180. https://doi.org/10.1021/es0108077.

Schmidl, C., Bauer, H., Dattler, A., Hitzenberger, R., Weissenboeck, G., Marr, I.L., Puxbaum, H., 2008. Chemical characterisation of particle emissions from burning leaves. Atmos. Environ. 42, 9070–9079. https://doi.org/10.1016/j.atmosenv.2008.09.010.

Simoneit, B.R.T., Cahill, T.A., Mazurek, M.A., 1980. Contamination of the Lake Tahoe air basin by high molecular weight petroleum residues. J. Air Pollut. Contr. Assoc. 30, 387–390. https://doi.org/10.1080/00022470.1980.10465954.

Šťávová, J., Stahl, D.C., Seames, W.S., Kubátová, A., 2012. Method development for the characterization of biofuel intermediate products using gas chromatography with simultaneous mass spectrometric and flame ionization detections. J. Chromatogr., A 1224, 79–88. https://doi.org/10.1016/j.chroma.2011.12.013.

Tao, J., Gao, J., Zhang, L., Zhang, R., Che, H., Zhang, Z., Lin, Z., Jing, J., Cao, J., Hsu, S.-C., 2014. PM$_{2.5}$ pollution in a megacity of southwest China: source apportionment and implication. Atmos. Chem. Phys. 14, 8679–8699. https://doi.org/10.5194/acp-14-8679-2014.

Tao, S., Yin, X., Jiao, L., Zhao, S., Chen, L., 2017. Temporal variability of source-specific solvent-extractable organic compounds in coastal aerosols over Xiamen, China. Atmosphere 8, 33. https://doi.org/10.3390/atmos8020033.

Tkacik, D.S., Presto, A.A., Donahue, N.M., Robinson, A.L., 2012. Secondary organic aerosol formation from intermediate-volatility organic compounds: cyclic, linear, and branched alkanes. Environ. Sci. Technol. 46, 8773–8781. https://doi.org/10.1021/es301112c.

Tsapakis, M., Lagoudaki, E., Stephanou, E.G., Kavouras, I.G., Koutrakis, P., Oyola, P., Baer, D.V., 2002. The composition and sources of PM$_{2.5}$ organic aerosol in two urban areas of Chile. Atmos. Environ. 36, 3851–3863. https://doi.org/10.1016/S1352-2310(02)00269-8.

van Drooge, B.L., Ballesta, P.P., 2009. Seasonal and daily source apportionment of polycyclic aromatic hydrocarbon concentrations in PM$_{10}$ in a semirural European area. Environ. Sci. Technol. 43, 7310–7316. https://doi.org/10.1021/es901381a.

Ventura, G.T., Schaeffer, P., 2007. Molecular evidence of Late Archean archaea and the presence of a subsurface hydrothermal biosphere. Proc. Natl. Acad. Sci. Unit. States Am. 104, 14260–14265. https://doi.org/10.1073/pnas.0610903104.

Ventura, G.T., Kenig, F., Reddy, C.M., Frysinger, G.S., Nelson, R.K., Mooy, B.V., Gaines, R.B., 2008. Analysis of unresolved complex mixtures of hydrocarbons extracted from Late Archean sediments by comprehensive two-dimensional gas chromatography (GC×GC). Org. Geochem. 39, 846–867. https://doi.org/10.1016/j.orggeochem.2008.03.006.

Viana, M., Amato, F., Alastuey, A., Querol, X., Moreno, T., García, D.S.S., Herce, M.D., Fernández-Patier, R., 2009. Chemical tracers of particulate emissions from commercial shipping. Environ. Sci. Technol. 43, 7472–7477. https://doi.org/10.1021/es901558t.

Wang, X.M., Ding, X., Fu, X.X., He, Q.F., Wang, S.Y., Bernard, F., Zhao, X.Y., Wu, D., 2012a. Aerosol scattering coefficients and major chemical compositions of fine particles observed at a rural site in the central Pearl River Delta, south China. J. Environ. Sci. (China) 24, 72–77. https://doi.org/10.1016/S1001-0742(11)60730-4.

Wang, Q.Q., Feng, Y.M., Huang, X.H.H., Griffith, S.M., Zhang, T., Zhang, Q.Y., Wu, D., Yu, J.Z., 2016. Nonpolar organic compounds as PM2.5 source tracers: investigation of their sources and degradation in the Pearl River Delta, China. J. Geophys. Res. Atmos. 121, 11862–11879. http://doi:10.1002/2016JD025315.

Wang, J.Z., Yang, Z.Y., Chen, T.H., 2012b. Source apportionment of sediment-associated aliphatic hydrocarbon in a eutrophicated shallow lake, China. Environ. Sci. Pollut. Res. 19, 4006–4015. https://doi.org/10.1007/s11356-012-0988-8.

Weitkamp, E.A., Sage, A.M., Pierce, J.R., Donahue, N.M., Robinson, A.L., 2007. Organic aerosol formation from photochemical oxidation of diesel exhaust in a smog chamber. Environ. Sci. Technol. 41, 6969–6975. https://doi.org/10.1021/es070193r.

White, H.K., Xu, L., Hartmann, P., Quinn, J.G., Reddy, C.M., 2013. Unresolved complex mixture (UCM) in coastal environments is derived from fossil sources. Environ. Sci. Technol. 47, 726–731. https://doi.org/10.1021/es3042065.

Woody, M.C., West, J.J., Jathar, S.H., Robinson, A.L., Arunachalam, S., 2015. Estimates of non-traditional secondary organic aerosols from aircraft SVOC and IVOC emissions using CMAQ. Atmos. Chem. Phys. 15, 6929–6942. https://doi.org/10.5194/acp-15-6929-2015.

Wu, Z.F., Zhang, Y.L., He, J.J., Chen, H.Z., Huang, X.L., Wang, Y.J., Yu, X., Yang, W.Q., Zhang, R.Q., Zhu, M., Li, S., Fang, H., Zhang, Z., Wang, X.M., 2019. Dramatic increase of reactive VOC emission from ships at berth after implementing the fuel switch policy in the Pearl River Delta Emission Control Area. Atmos. Chem. Phys. Discuss. 2019, 1–25. http://dio.org/10.5194/acp-2019-897.

Xie, M., Barsanti, K.C., Hannigan, M.P., Dutton, S.J., Vedal, S., 2013. Positive matrix factorization of PM$_{2.5}$-eliminating the effects of gas/particle partitioning of semivolatile organic compounds. Atmos. Chem. Phys. 13, 7381–7393. https://doi.org/10.5194/acp-13-7381-2013.

Xie, M., Hannigan, M., Barsanti, K., 2014. Gas/particle partitioning of n-alkanes, PAHs and oxygenated PAHs in urban Denver. Atmos. Environ. 95, 355–362. https://doi.org/10.1016/j.atmosenv.2014.06.056.

Yan, X.Y., Ohara, T., Akimoto, H., 2006. Bottom-up estimate of biomass burning in mainland China. Atmos. Environ. 40, 5262–5273. https://doi.org/10.1016/j.atmosenv.2006.04.040.

Yu, X., Yu, Q.Q., Zhu, M., Tang, M.J., Li, S., Yang, W.Q., Zhang, Y.L., Deng, W., Li, G., Yu, Y.G., Huang, Z.H., Song, W., Ding, X., Hu, Q.H., Li, J., Bi, X.H., Wang, X.M., 2017. Water soluble organic nitrogen (WSON) in ambient fine particles over a megacity in south China: spatiotemporal variations and source apportionment. J. Geophys. Res. Atmos. 122, 13045–13060. https://doi.org/10.1002/2017JD027327.

Zhang, Y.X., Dou, H., Chang, B., Wei, Z.C., Qiu, W.X., Liu, S.Z., Liu, W.X., Tao, S., 2008. Emission of polycyclic aromatic hydrocarbons from indoor straw burning and emission inventory updating in China. Ann. N. Y. Acad. Sci. 1140, 218–227. https://doi.org/10.1196/annals.1454.006.

Zhang, Y.S., Shao, M., Lin, Y., Luan, S.J., Mao, N., Chen, W.T., Wang, M., 2013. Emission inventory of carbonaceous pollutants from biomass burning in the Pearl River Delta Region, China. Atmos. Environ. 76, 189–199. https://doi.org/10.1016/j.atmosenv.2012.05.055.

Zhang, Y.L., Wang, X.M., Li, G.H., Yang, W.Q., Huang, Z.H., Zhang, Z., Huang, X.Y., Deng, W., Liu, T.Y., Huang, Z.Z., Zhang, Z.Y., 2015. Emission factors of fine particles, carbonaceous aerosols and traces gases from road vehicles: recent tests in an urban

tunnel in the Pearl River Delta, China. Atmos. Environ. 122, 876–884. https://doi.org/10.1016/j.atmosenv.2015.08.024.

Zhao, Y.L., Hennigan, C.J., May, A.A., Tkacik, D.S., de Gouw, J.A., Gilman, J.B., Kuster, W.C., Borbon, A., Robinson, A.L., 2014. Intermediate-volatility organic compounds: a large source of secondary organic aerosol. Environ. Sci. Technol. 48, 13743–13750. https://doi.org/10.1021/es5035188.

Zhao, Y.L., Nguyen, N.T., Presto, A.A., Hennigan, C.J., May, A.A., Robinson, A.L., 2015. Intermediate volatility organic compound emissions from on-road diesel vehicles:

chemical composition, emission factors, and estimated secondary organic aerosol production. Environ. Sci. Technol. 49, 11516–11526. http://dio.org/10.1021/acs.est.5b02841.

Zhao, B., Wang, S.X., Donahue, N.M., Jathar, S.H., Huang, X.F., Wu, W.J., Hao, J.M., Allen, L.R., 2016. Quantifying the effect of organic aerosol aging and intermediate-volatility emissions on regional-scale aerosol pollution in China. Sci. Rep. 6 https://doi.org/10.1038/srep28815.